Naturally Phase-Matched Second-Harmonic Generation in a Whispering-Gallery-Mode Resonator

J. U. Fürst,[1,2] D. V. Strekalov,[1,3] D. Elser,[1,2] M. Lassen,[1,4] U. L. Andersen,[1,4] C. Marquardt,[1,2] and G. Leuchs[1,2]

[1]*Max Planck Institute for the Science of Light, Erlangen, Germany*
[2]*Department of Physics, University of Erlangen-Nuremberg, Germany*
[3]*Jet Propulsion Laboratory, California Institute of Technology, Pasadena, California, USA*
[4]*Department of Physics, Technical University of Denmark, Kongens Lyngby, Denmark*
(Received 19 December 2009; published 12 April 2010)

We demonstrate for the first time natural phase matching for optical frequency doubling in a high-Q whispering-gallery-mode resonator made of lithium niobate. A conversion efficiency of 9% is achieved at 30 μW in-coupled continuous wave pump power. The observed saturation pump power of 3.2 mW is almost 2 orders of magnitude lower than the state-of-the-art value. This suggests an application of our frequency doubler as a source of nonclassical light requiring only a low-power pump, which easily can be quantum noise limited. Our theoretical analysis of the three-wave mixing in a whispering-gallery-mode resonator provides the relative conversion efficiencies for frequency doubling in various modes.

Various types of oscillations can be enhanced by appropriate resonators. Examples range from resonating chambers for sound waves to cavities for electromagnetic waves. Nonlinear cross-coupling of different oscillations can be enhanced as well, e.g., between optical waves, between optical and radio-frequency electromagnetic waves, and between mechanical and optical oscillations [1].

A resonator of particular interest in the context of quantum and nonlinear optics is the whispering-gallery-mode resonator (WGMR). In WGMRs, light is guided via continuous total internal reflection. The small mode volume combined with the absence of external reflecting elements provides for a very high quality factor Q and good spatial localization of the optical fields. Moreover, the WGMR enables us to continuously control the coupling strength between the intracavity modes and the modes outside the cavity. This capability may be compared to a cavity mirror with continuously variable reflectivity.

Because of these unique capabilities, various nonlinear processes have been observed in WGMRs, including four wave mixing [2–5], Raman [5,6], parametric [7] and Brillouin [8] scattering, microwave upconversion [9], second [10] and third [11] harmonic generation. Furthermore, a plethora of dynamic effects has been predicted and observed in the cavities with the second order nonlinear response, examples being bistability, chaotic behavior, and self-pulsing [12], along with nonclassical effects such as squeezing and entanglement [13]. It is intriguing to investigate these effects in a highly efficient WGMR.

In this Letter we report on the second harmonic (SH) generation in a doubly resonant WGMR. We employ noncritical type-I phase matching, and achieve the SH conversion efficiency of 9% at 30 μW pump power. This is nearly 2 orders of magnitude higher than the previous state-of-the-art result for the same pump power, obtained with a less

efficient quasi–phase matching [10]. At higher pump power, the conversion efficiency saturates.

The phase-matching conditions for SH and degenerate parametric down-conversion (PDC) reflect the conservation laws associated with the resonator symmetries. They arise from the interaction Hamiltonian

$$H_{\text{int}} = \int \chi^{(2)} E_s (E_p^\dagger)^2 dV + \text{H.c.} \tag{1}$$

expressed via the effective quadratic nonlinearity $\chi^{(2)}$ and the pump and SH positive frequency electric field operators E_p and E_s. In Cartesian coordinates, the integral in (1) gives rise to three momentum conservation equations: $2\vec{k}_p = \vec{k}_s$. In a spherical WGMR, a mode is defined by a set of polar, azimuthal, and radial numbers $\{L, m, q\}$. Assuming that the WGMR radius R is much larger than the optical wavelength λ, such that there is no coupling disturbance, and that the WGMs are near equatorial, we can reduce the electric fields in both polarizations to a scalar eigenfunction [14] with a scaling factor E_0:

$$E_{Lmq}(r, \theta, \phi) = E_0 Y_{Lm}(\theta, \phi) j_L(k_{Lq} r). \tag{2}$$

The angular part of (2) is a spherical harmonic

$$Y_{Lm}(\theta, \phi) = \sqrt{\frac{(2L+1)(L-m)!}{4\pi(L+m)!}} P_L^m(\cos\theta) e^{im\phi}, \tag{3}$$

where $P_L^m(\cos\theta)$ are the associated Legendre polynomials. The radial wave number k_{Lq} in the argument of the spherical Bessel function $j_L(k_{Lq} r)$ relates the WGM eigenfrequency ω to L and q via the dispersion equation

$$k_{Lq} = \omega \frac{n}{c} = \frac{L}{R}[1 + \alpha_q (2L^2)^{-1/3} + O(L^{-1})], \tag{4}$$

where n is the material index of refraction and α_q is the qth zero of the Airy function [14,15].

Applying (1) to the angular part of (2) yields the Clebsch-Gordan coefficients whose subscripts s and p refer to the pump and the second harmonic, respectively:

$$\langle L_p, L_p; m_p, m_p | L_s, m_s \rangle = \int Y_{L_s m_s}^*(\theta, \phi) Y_{L_p m_p}^2(\theta, \phi)$$
$$\times \sin\theta d\theta d\phi. \qquad (5)$$

Selection rules for Clebsch-Gordan coefficients are

$$m_s = 2m_p, \qquad L_s \leq 2L_p. \qquad (6)$$

The first condition in (6) is conservation of the azimuthal component of the orbital momentum, while the second one arises from the triangular condition for a vector sum of the orbital momenta of two pump photons. The phase-matching conditions for the SH generated on a *surface* of a spherical WGMR have been already construed as the addition rules for the orbital momenta [14]. This also applies to our WGMR, and the Clebsch-Gordan factors (5) in the conversion efficiency emphasize the analogy with atomic systems. Notice that a spectrum of a spherical WGMR (4) is degenerate with respect to m, which decouples the first selection rule of (6) from the frequency-doubling resonance condition

$$\omega_s = 2\omega_p \qquad (7)$$

and makes the phase matching easier to satisfy.

The relative SH conversion efficiencies for different WGMs are found from Eq. (5) using Gaunt's formula [16] and treating large factorials in Stirling's approximation. Remarkably, for L and m sufficiently large for dispersion Eq. (4) to remain a good approximation (which is the case in our experiment), the coefficients (5) normalized to $\langle m, m; m, m | 2m, 2m \rangle$ are practically independent of m and therefore of R and λ. This normalization coefficient describes nonlinear coupling of two equatorial modes ($L = m$). The equatorial modes have a single antinode at $\theta = \pi/2$ and therefore yield the best coupling of the WGMR with the free-space modes, as well as the best overlap with other equatorial modes. To describe nonequatorial modes, we introduce $\nu_p \equiv L_p - m_p \geq 0$ and $\nu_s \equiv L_s - m_s \geq 0$. The normalized Clebsch-Gordan coefficients are shown in Fig. 1. From this figure we see that the second selection rule of (6) breaks the symmetry between the SH and degenerate PDC processes. While the former can couple an equatorial pump only to another equatorial mode, the latter can couple the equatorial pump to a variety of modes.

The radial part of integral (1) with substituted (2) and (4) is evaluated approximating the large-order Bessel functions by Airy functions. The results are normalized to the $\{\omega_p, q_p = 1\} \rightarrow \{2\omega_p, q_s = 1\}$ coupling coefficient, and shown in Fig. 2. These coefficients are practically independent of L_p and L_s and therefore of R and λ. The relative
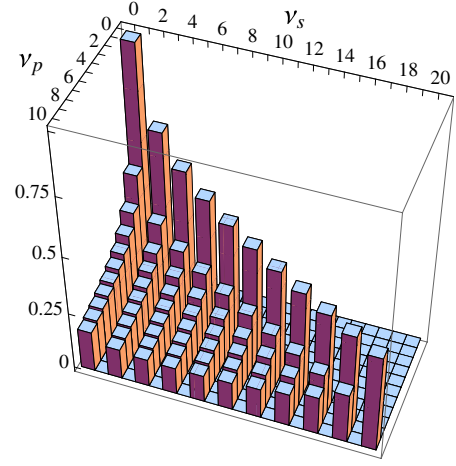

FIG. 1 (color online). Normalized Clebsch-Gordan coefficients $\langle m + \nu_p, m + \nu_p; m, m | 2m + \nu_s, 2m \rangle / \langle m, m; m, m | 2m, 2m \rangle$.

efficiencies of different conversion channels $\{\omega_p, L_p, m_p, q_p\} \rightarrow \{2\omega_p, L_s, 2m_p, q_s\}$ are found as a product of squares of coefficients from Figs. 1 and 2.

Our experimental setup is shown in Fig. 3. The WGMR is made from a congruent 5% MgO-doped lithium niobate z-cut wafer. Its radius is $R = 1.9$ mm and height is approximately 0.5 mm. The rim of the disk is polished into a tapered shape that near the equator can be approximated as a spheroid with radii R and ρ. Their ratio $R/\rho \approx 7.5$ is nearly optimal [9] for coupling of the horizontally polarized pump.

The pump is a free-space Gaussian beam from a continuous wave Nd:YAG laser (InnoLight Mephisto) with a wavelength of 1064 nm. It is focused by a microscope objective onto the back side of a diamond prism at an angle that allows for total internal reflection. The resonator is placed near the reflected beam's footprint, so that the coupling occurs via frustrated total internal reflection. The coupling is varied by changing the gap between the prism and the resonator rim. The disk and the prism are mounted
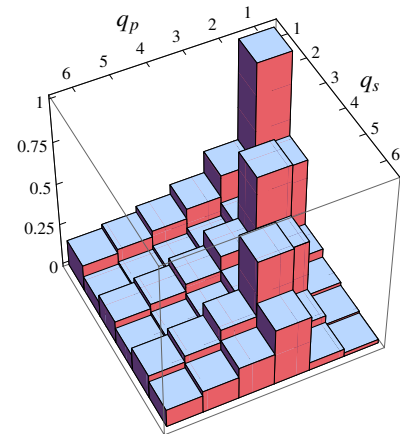

FIG. 2 (color online). Normalized absolute-value coupling coefficients for frequency doubling $\{\omega_p, q_p\} \rightarrow \{2\omega_p, q_s\}$.
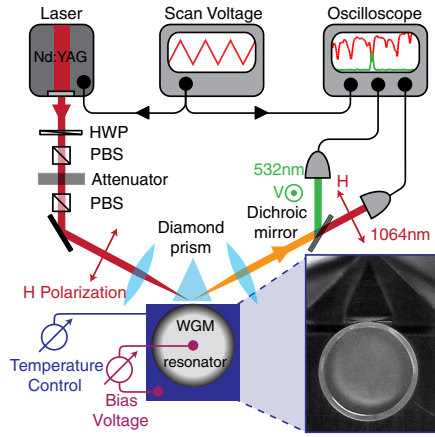
FIG. 3 (color online).   Experimental setup.

on a hot plate whose temperature is stabilized. The hori-
zontally polarized pump couples to the ordinary polarized
modes of the resonator, and the vertically polarized SH is
generated into an extraordinary polarized mode. Light
coupled out of the disk is recollimated by another objec-
tive, and the fundamental and the SH components are
separated by a dichroic mirror and focused onto photo-
detectors. Finally, the signals are monitored by an
oscilloscope.

Scanning the laser frequency we observe the pump
transmission, which reveals the WGM spectrum at the
fundamental wavelength (see Fig. 4). Fitting the reso-
nances with a Lorentzian function we find a minimal
linewidth $\gamma = 8.3$ MHz, $(Q = 3.4 \times 10^7)$, and a maxi-
mum contrast of 90%, for a critically coupled resonator.

An electrode attached to the disk allows us to apply a
bias voltage to the resonator. The bias shifts the ordinary
(pump) and extraordinary (signal) mode frequencies ω_p
and ω_s differently, proportionally to the electro-optic co-
efficients r_{31} and $r_{33} \approx 3.2r_{31}$, respectively. This differen-
tial frequency tuning of WGMs allows us to achieve
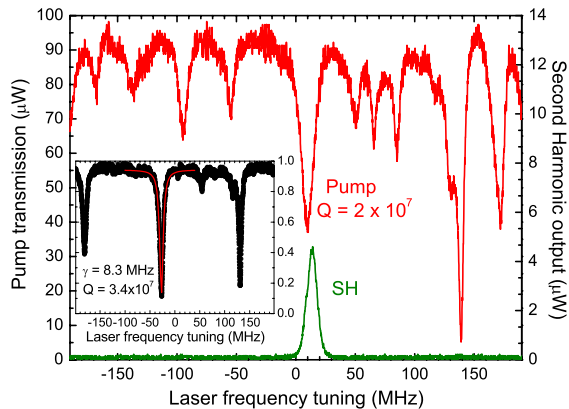condition (7) required for the frequency doubling.

FIG. 4 (color online).   Transmitted pump power and the SH
signal. The coupling is optimized for high SH output, which
corresponds to overcoupled fundamental modes. On the inset: a
typical WGM spectrum of a critically coupled resonator.

Changing the resonator temperature has the same effect
as changing the bias voltage, since the temperature depen-
dences of the indices of refraction $n_o(T)$ and $n_e(T)$ are
different. While the electro-optical tuning is faster, the
temperature tuning has a larger dynamic range.

To find the phase-matching temperature for the WGMR,
we made a bulk crystal from the same wafer and deter-
mined its phase-matching temperature to be 121.7 °C. This
result was consistent with the calculations based on the
Sellmeier equation [17] and with an earlier experiment
[18]. Using the Sellmeier equation together with the
spherical WGMR dispersion (4), we calculated the optimal
phase-matching temperature to be 94.1 °C. We assumed
$\omega_p = 2\pi c/1064.3$ nm, $m_p \approx 25\,200$, and $q_s = q_p = 1$,
as this is the most efficient conversion channel within the
accessible temperature and wavelength ranges.

We find the phase matched modes by frequency tuning
the extraordinary WGMs at 532 nm relative to the ordinary
WGMs at 1064 nm with the bias voltage. We compensate
for the frequency shift of the fundamental WGM by the
laser central frequency. At some bias voltages the require-
ment (7) is occasionally satisfied for a pair of modes. Then
if Eq. (6) is also satisfied, SH is generated, see Fig. 4. For
different pump modes this might happen once or several
times. However, for the majority of the modes it never
happens within the explored parameter space.

We observed different conversion efficiency for different
WGMs. Figure 5 shows the best measured conversion
efficiency as a function of the in-coupled pump power. It
is worth noting that the *detected* SH power is proportional
to the power *circulating* in the resonator and to the reso-
nator coupling. The circulating power, on the other hand, is
reduced when the coupling increases (due to decreasing Q
factors). As a result, the detected SH power as a function of
the coupling has a maximum which corresponds to the
over-coupled fundamental WGM.

The theoretical model for the SH generation [19] in an
idealized doubly resonant WGMR has been advanced in
[10]. A key parameter in this model is the saturation power
W_0 which can be considered as an absolute measure of the
nonlinear conversion efficiency, independent of the pump
power. The experimental value of W_0 reported in [10] is
300 mW. We have measured $W_0 = 3.2$ mW, see Fig. 5.
However, even this low power greatly exceeds the theo-
retical estimate of $W_0 \approx 6$ μW derived for our resonator
based on the theoretical model in Ref. [10]. This indicates
that the spatial overlap between the SH and fundamental
WGMs in our experiment deviated from the optimal one by
a factor of $\sqrt{W_0(\text{theor})/W_0(\text{expt})} \approx 0.043$. To explain this
discrepancy we point out that the diagonal coupling coef-
ficients $L_s = 2L_p$ in Fig. 1 decrease rather slowly with
increasing L-m. Also, according to Fig. 2, coupling be-
tween WGMs with different radial numbers q remains
significant even when the difference is large. Therefore
we observe multiple instances of phase matching with
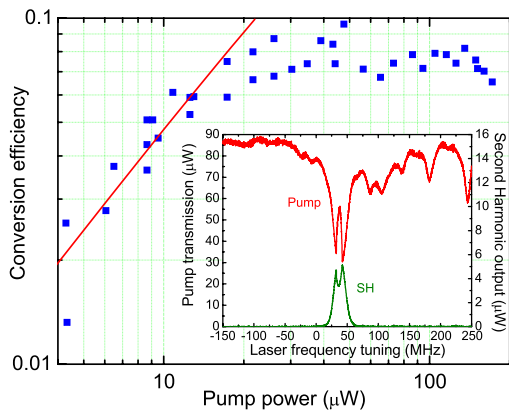nonoptimal conversion efficiencies and consequently

FIG. 5 (color online).   SH conversion efficiency as a function of the in-coupled power: experimental data and theoretical fit [10] corresponding to the saturation pump power $W_0 = 3.2$ mW. On the inset: transmitted pump power and the second harmonic signal above the "self-limiting" threshold which arises at a much lower power than W_0.

higher saturation power W_0, than for optimal conditions. It is difficult to uniquely establish which pair of modes yielded the overlap factor inferred from experiment.

Similar nonoptimal conversion efficiencies were measured in the range of 94 °C to 122 °C. Evidently, the calculations based on the spherical WGMR dispersion (4) have not been sufficiently accurate for our nonspherical resonator. Considering a very narrow temperature width of a WGMR phase matching, of the order of 0.001 °C, empirically searching for the optimal phase matching within a 30° temperature range was cumbersome. A more accurate initial temperature estimate is preferable.

The conversion efficiencies measured both in [10] and here (see Fig. 5) reach the maxima and saturate at much lower in-coupled pump powers than W_0. We attribute this to a nonlinear "self-limiting" effect arising when the circulating pump power exceeds a certain threshold, see the inset in Fig. 5. This effect is not related to the photo-refractive damage (which can also be observed in our resonator, see [20]). While the photorefractive damage causes quasipermanent changes to the WGM spectra, the "self-limiting" effect shows purely dynamic behavior as a function of the pump power and coupling. This effect may be related to the onset of self-pulsing or similar dynamics [12] and will be discussed elsewhere.

In summary, we present the first natural noncritical type-I phase matching for 1064 to 532 nm optical frequency doubling in a high-Q WGMR. This results in a hundredfold lower saturation pump power. Our theoretical study of phase matching in the spherical geometry of WGMRs has predicted the existence of multiple coupled WGM pairs with varying conversion efficiency consistent with our observations. The study also predicted the asymmetry between the SH and PDC selection rules, which may lead

to the competition between these processes and explain the observed "self-limiting" effect.

The best efficiency of 9% was achieved at 30 μW in-coupled cw pump power. Such a high-efficiency low-power frequency conversion process is very interesting in the context of nonlinear optomechanical coupling [1], nonlinear dynamics [12], and quantum optics [13]. Experiments with linear cavities showed reduction of amplitude noise below the quantum limit at the fundamental [21] and SH [18] frequencies. The theoretical limit for this reduction has been shown [22] to be determined by the pump noise. In the low pump power regime, shot noise and subshot noise pump light fields are easily accessible, see, e.g., [23]. We plan to exploit the low-power operation regime in nonlinear WGMRs to lift the pump noise limitation and to realize a source of nonclassical light.

[1] See, e.g., G. Anetsberger *et al.*, Nat. Photon. **2**, 627 (2008); F. Marquardt and S. M. Girvin, Physics **2**, 40 (2009).
[2] A. A. Savchenkov *et al.*, Phys. Rev. Lett. **93**, 243905 (2004).
[3] T. J. Kippenberg, S. M. Spillane, and K. J. Vahala, Phys. Rev. Lett. **93**, 083904 (2004).
[4] P. Del'Haye *et al.*, Nature (London) **450**, 1214 (2007).
[5] A. A. Savchenkov *et al.*, Phys. Rev. Lett. **101**, 093902 (2008).
[6] S. M. Spillane *et al.*, Nature (London) **415**, 621 (2002).
[7] A. A. Savchenkov *et al.*, Opt. Lett. **32**, 157 (2007).
[8] I. S. Grudinin, A. B. Matsko, and L. Maleki, Phys. Rev. Lett. **102**, 043902 (2009).
[9] D. V. Strekalov *et al.*, Opt. Lett. **34**, 713 (2009).
[10] V. S. Ilchenko *et al.*, Phys. Rev. Lett. **92**, 043903 (2004).
[11] T. Carmon and K. J. Vahala, Nature Phys. **3**, 430 (2007).
[12] P. D. Drummond *et al.*, Opt. Acta **27**, 321 (1980); M. Bache *et al.*, Phys. Rev. A **65**, 033811 (2002).
[13] P. D. Drummond *et al.*, Opt. Acta **28**, 211 (1981); A. Heidmann *et al.*, Phys. Rev. Lett. **59**, 2555 (1987).
[14] G. Kozyreff, J. L. Dominguez Juarez, and Jordi Martorell, Phys. Rev. A **77**, 043817 (2008).
[15] V. S. Ilchenko *et al.*, J. Opt. Soc. Am. A **20**, 157 (2003).
[16] J. A. Gaunt, Phil. Trans. R. Soc. A **228**, 151 (1929).
[17] U. Schlarb and K. Betzler, Phys. Rev. B **50**, 751 (1994).
[18] A. Sizmann *et al.*, Opt. Commun. **80**, 138 (1990).
[19] In Eq. (5) of [10], both $\sqrt{S(1+S)}$ should be replaced by $\sqrt{S(2+S)}$. A. B. Matsko (private communication).
[20] A. A. Savchenkov *et al.*, Appl. Phys. Lett. **88**, 241909 (2006).
[21] S. F. Pereira *et al.*, Phys. Rev. A **38**, 4931 (1988).
[22] A. G. White *et al.*, J. Opt. Soc. Am. B **13**, 1337 (1996).
[23] M. Lassen *et al.*, Opt. Express **15**, 5077 (2007).